THERMAL CONVECTION IN TURBULENT FLOW, IMAGE SYNTHESIS AND HEAT ANIMATION

Didier Arquès, Eric Felgines, Sylvain Michelin, Karine Zampieri

Equipe de synthèse d'images, Institut Gaspard Monge
Université de Marne la Vallée - 5, boulevard Descartes - Champs sur Marne
77454 Marne la Vallée CEDEX 2
France
{arques,felgines,michelin}@univ-mlv.fr, K.Zampieri@univ-mulhouse.fr

ABSTRACT

This paper focuses on realistic ray-tracing rendering of scenes which integrate participating media. We work on the temperature sensitive index of refraction, in order to deflect the rays' path and thus visualize a scene through heat. We can also visualize three-dimensional convective motions, under the shape of fumes. In this respect, we suggest to solve the NS (Navier-Stokes) equations through a simple approach, which offers better steadiness than classical methods, and which is easy to implement. We are considering the three-dimensional and turbulent case of this system, combined with the energy equation, in order to obtain incompressible fluid or gaseous realistic participating media.

Keywords: ray-tracing, numerical simulation, heat transfer convection.

1. INTRODUCTION

For 15 years, research in the field of image synthesis has been directing towards methods based on physical models. Numerical simulation has been really increasing and radiosity [1] was introduced in 1984. When considering the different existing modes of heat transfer, this corresponds to radiation. However, in studying heat transfers, we get used to distinguish a particular mode called convection, which itself is linked to a specific physical process. In the field of image synthesis, a lot of studies suggest methods built upon statistical equations, in order to generate natural phenomena. In 1997, Nick Foster [2] was the first one to bring a solution for solving the equations of the convection describing the motion of a hot newtonian fluid. He referred to Francis H. Harlow’s paper [3] on fluids’ dynamics (1965). Section 2 of this paper deals with the fundamental principles of convection heat transfer through the related system of conservation equations. The third section expounds one of the most classical methods for resolving this system, and then discusses its limits, while bringing in the problems that are inherent to the obtaining of a turbulent solution of these equations. In section 4, a slight supplement to this method shall improve steadiness, especially in the case of important velocity variations. The last section shows different possibilities of rendering - after calculations are made - , as for example, visualizing something through heat, simulating fumes,…

2. FUNDAMENTAL PRINCIPLES OF CONVECTION HEAT TRANSFERS

Convection [4] is a mode of heat transfer, which appears when a moving fluid shows temperature spatial inhomogeneities. We want to determine, - at all points and at every moment -, the fluid's characteristic measurements (velocity, pressure, temperature). To be clearer, we will show the mechanical and thermodynamical conservation principles on a two-dimensional plan. Three-dimensional equations are built in the same way [4].

2.1 Mass conservation (MC)

In a given system, there is MC if there is no mass creation. Let us suppose a fluid's elementary volume as $\Delta x \Delta y$ (*fig. 1*), velocity's components as u and v, and density as ρ. MC will be translated into :

$$\partial(\rho\Delta x\Delta y)/\partial t = \rho u\Delta y + \rho v\Delta x - \left[\rho u + \Delta x\partial(\rho u)/\partial x\right]\Delta y - \left[\rho v + \Delta y\partial(\rho v)/\partial y\right]\Delta x \qquad (1)$$

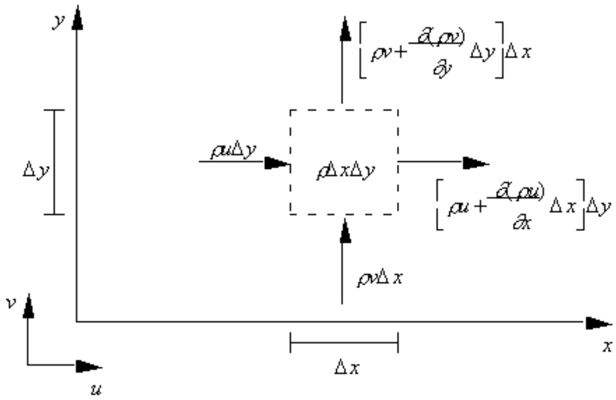

Figure 1. Mass conservation

When dividing (1) by $\Delta x\Delta y$ and considering density's time and space negligible variations - compared to the local velocity variations -, the equation (1) is reduced to zero velocity vector divergence :

$$\nabla \cdot V = 0 \qquad (2)$$

2.2 Momentum equation (ME)

ME is expressed like $\text{mass} \times \text{velocity}$. This is an impulse. *Figure 2* shows the forces, which apply to an elementary volume : the figure on the top represents the forces that are connected to the flow's motions on x, whereas the figure on the bottom represents usual forces : normal tension σ_x (pressure), tangential tension τ_{xy} (viscosity) and body force F_X :

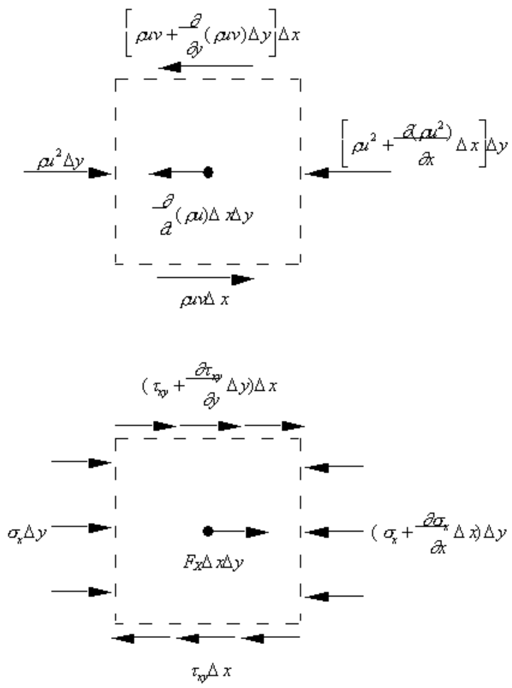

Figure 2. Momentum conservation

Projecting these forces on Ox brings one of the NS components. In accordance with (1) and referring to [4], viscosity's constant coefficient of the fluid μ is defined by $\sigma_x = P - 2\mu(\partial u/\partial x) + 2\mu(\partial u/\partial x + \partial v/\partial y)/3$ and $\tau_{xy} = \mu(\partial u/\partial y + \partial v/\partial x)$, where P is the pressure force. Consequently, ME is written on all the axes as :

$$\rho\frac{DV}{Dt} = -\nabla P + \mu\nabla^2 V + F \qquad (3)$$

where D/Dt is the $\partial/\partial t + u\partial/\partial x + v\partial/\partial y$ operator. A convection system will consider F as an upward force, which is due to heat. Boussinesq's approximation [4] defines $F_y = g\beta(T - T_0)$, where β is the thermal expansion coefficient and T_0 the reference temperature. For the fluid's constant density $\rho = \rho_0$, (2) and (3) are building the complete NS equations governing the motion of an incompressible newtonian fluid.

2.3 Energy conservation (EC)

Equations (2) and (3) shall imply the resolution of a system, where unknowns are velocity's components and pressure. As we are mainly interested in heat distribution through a fluid, we shall associate this system with the first principle of thermodynamics (energy equation), which, in terms of temperature, is written as [4] :

$$\rho c_p \frac{DT}{Dt} = \nabla\cdot(k\nabla T) + q + \beta T\frac{DP}{Dt} + \mu\Phi$$

where c_p shall represent specific heat, T temperature, k thermal conductivity, q rate of internal heat generation, β thermal expansion coefficient, and Φ the dissipation function, which is bound to the energy degradation in heat (viscous frictions). Most of the convection problems will consider $q = 0$, negligible viscous dissipation $\mu\Phi$ and compressibility effect $\beta TDP / Dt$. In this simplified model :

$$\frac{DT}{Dt} = \alpha \nabla^2 T \tag{4}$$

where $\alpha = \dfrac{k}{\rho c_p}$ is the thermal diffusion coefficient.

3. CLASSICAL METHOD FOR SOLVING THERMAL CONVECTION EQUATIONS

Most of the convection problems are solved by the finite volume method [5], which shall discretize equations on an axisymmetrical mesh, from their integral expression. On the basis of a uniform mesh, the method is reduced to a finite difference expression. We will present, in this case, the system's resolution on a three-dimensional voxmap, where each voxel is defined by a Δx width, a Δy height, a Δz depth and contains a velocity, pressure and temperature value.

3.1 Discretization scheme for the evolution equations

Section 2 presented the fundamental principles of the convection equations. Being fundamentally three-dimensional, expressions (2)-(4) shall build :

$$\frac{\partial u}{\partial x} + \frac{\partial v}{\partial y} + \frac{\partial w}{\partial z} = 0 \tag{5}$$

$$\frac{\partial u}{\partial t} + \frac{\partial u^2}{\partial x} + \frac{\partial}{\partial y}(uv) + \frac{\partial}{\partial z}(uw) = -\frac{1}{\rho_0}\frac{\partial P}{\partial x} + \nu_0\left(\frac{\partial^2 u}{\partial x^2} + \frac{\partial^2 u}{\partial y^2} + \frac{\partial^2 u}{\partial z^2}\right) \tag{6}$$

$$\frac{\partial v}{\partial t} + \frac{\partial}{\partial x}(uv) + \frac{\partial v^2}{\partial y} + \frac{\partial}{\partial z}(vw) = -\frac{1}{\rho_0}\frac{\partial P}{\partial y} + \nu_0\left(\frac{\partial^2 v}{\partial x^2} + \frac{\partial^2 v}{\partial y^2} + \frac{\partial^2 v}{\partial z^2}\right) + \frac{g\beta}{\rho_0}(T - T_0) \tag{7}$$

$$\frac{\partial w}{\partial t} + \frac{\partial}{\partial x}(uw) + \frac{\partial}{\partial y}(vw) + \frac{\partial w^2}{\partial z} = -\frac{1}{\rho_0}\frac{\partial P}{\partial z} + \nu_0\left(\frac{\partial^2 w}{\partial x^2} + \frac{\partial^2 w}{\partial y^2} + \frac{\partial^2 w}{\partial z^2}\right) \tag{8}$$

$$\frac{\partial T}{\partial t} + \frac{\partial}{\partial x}(uT) + \frac{\partial}{\partial y}(vT) + \frac{\partial}{\partial z}(wT) = \alpha_0\left(\frac{\partial^2 T}{\partial x^2} + \frac{\partial^2 T}{\partial y^2} + \frac{\partial^2 T}{\partial z^2}\right) \tag{9}$$

where (u, v, w, T, P) are respectively velocity (3 coordinates), temperature and pressure unknowns. Cinematic viscosity coefficient $\nu_0 = \mu / \rho_0$, g, β, T_0, and $\alpha_0^{-1} = \rho_0 c_P / k$ are constant parameters. The expression $g\beta(T - T_0)$ is added here as a classical force. We can add to the system as many forces as wished, to undergo stream effect, Coriolis effects… In terms of finite differences [6], spatial discretization of these equations applies a Taylor development for each of the differential terms. Following is the main scheme used for all the types of spatial terms of the (5)-(9) equations :

$$\left[\frac{\partial u}{\partial x}\right]_{i,j,k} = \frac{u_{i,j,k} - u_{i-1,j,k}}{\Delta x}$$

$$\left[\frac{\partial u^2}{\partial x}\right]_{i,j,k} = \frac{u^2_{i+1,j,k} - u^2_{i-1,j,k} + 2u_{i,j,k}\left(u_{i+1,j,k} - u_{i-1,j,k}\right)}{4\Delta x}$$

$$\left[\frac{\partial}{\partial y}(uv)\right]_{i,j,k} = \frac{\left(u_{i,j,k} + u_{i,j+1,k}\right)\left(v_{i+1,j,k} + v_{i,j,k}\right) - \left(u_{i,j-1,k} + u_{i,j,k}\right)\left(v_{i,j-1,k} + v_{i+1,j-1,k}\right)}{4\Delta y}$$

$$\left[\frac{\partial P}{\partial x}\right]_{i,j,k} = \frac{P_{i+1,j,k} - P_{i,j,k}}{\Delta x}$$

$$\left[\frac{\partial^2 u}{\partial x^2}\right]_{i,j,k} = \frac{u_{i+1,j,k} - 2u_{i,j,k} + u_{i-1,j,k}}{\Delta x^2}$$

$$\left[\frac{\partial}{\partial x}(uT)\right]_{i,j,k} = \frac{u_{i,j,k}\left(T_{i,j,k} + T_{i+1,j,k}\right) - u_{i-1,j,k}\left(T_{i,j,k} + T_{i-1,j,k}\right)}{2\Delta x}$$

where $[\partial u / \partial x]_{i,j,k}$ shall represent the discrete expression of the first derivative of u according to x for the (i, j, k) coordinates' voxel. From the spatial discretization, remains a relation of $dQ / dt = \Psi(Q)$ type, where Q is a discrete quantity corresponding to velocity or temperature. The usual method of time integration of this differential system is the explicit Euler method :

$$Q^{n+1} = Q^n + \Delta t \Psi\left(Q^n\right) \tag{10}$$

It brings Q's solution at $n+1$ time step by following the solution's slope at n time step. We will usually resolve (10) in an iterative manner.

3.2 Classical resolution of the complete system

At each time step, new velocity and pressure values are updated by a "ping-pong" strategy. It discretizes the (5) equation's velocity terms and the (6)-(8) equations' pressure terms at $n+1$ time step, and all the other spatial terms at n time step :

$$\frac{u_{i,j,k}^{n+1}-u_{i-1,j,k}^{n+1}}{\Delta x}+\frac{v_{i,j,k}^{n+1}-v_{i,j-1,k}^{n+1}}{\Delta y}+\frac{w_{i,j,k}^{n+1}-w_{i,j,k-1}^{n+1}}{\Delta z}=0 \tag{5d}$$

$$u_{i,j,k}^{n+1}=u_{i,j,k}^{n}+\Delta t\left(f_u(u,v,w)_{i,j,k}^{n}-\frac{1}{\rho_0\Delta x}\left(P_{i+1,j,k}^{n+1}-P_{i,j,k}^{n+1}\right)\right) \tag{6d}$$

$$v_{i,j,k}^{n+1}=v_{i,j,k}^{n}+\Delta t\left(f_v(u,v,w)_{i,j,k}^{n}-\frac{1}{\rho_0\Delta y}\left(P_{i,j+1,k}^{n+1}-P_{i,j,k}^{n+1}\right)+\left[\frac{g\beta}{\rho_0}\left(T_{i,j,k}^{n}-T_0\right)\right]\right) \tag{7d}$$

$$w_{i,j,k}^{n+1}=w_{i,j,k}^{n}+\Delta t\left(f_w(u,v,w)_{i,j,k}^{n}-\frac{1}{\rho_0\Delta z}\left(P_{i,j,k+1}^{n+1}-P_{i,j,k}^{n+1}\right)\right) \tag{8d}$$

$$T_{i,j,k}^{n+1}=T_{i,j,k}^{n}+\Delta t.\,f_T(u,v,w,T)^{n} \tag{9d}$$

where $u_{i,j,k}^{n+1}$ represents the x component value of the velocity from the (i,j,k) voxel, at the resolution's $n+1$ iteration, and where f_u, f_v, f_w and f_T are known functions (n time step). When n is equal to 0 (time t_0), those are defined by initial conditions. Resolution of the velocity/pressure (NS) system can be effected by the usual mathematics of partial derivative equations (PDE), which allows to consider classical forces and the energy equation separately. (i) Temperature is explicitly determined at the beginning of each time step. (ii) Substituting the terms of (5d) by the (6d)-(8d) expressions without considering the quantity between brackets, will give the Poisson equation :

$$\Delta P_{i,j,k}^{n+1}=\frac{\rho_0}{\Delta t}\varphi(u,v,w)^{n} \tag{11}$$

where the $\varphi(u,v,w)^n$ function is known. Thus, MC is valid in the whole system and (11) shall be resolved by an usual iterative method, which shall determine a value for P^{n+1} in each voxel. (iii) Its injection in (6d)-(8d) shall bring u, v and w up-to-date. The (i)-(iii) process is reiterated up to convergence, which can be assured by imposing limits conditions to the calculation field. The physical limit shall be interpreted as a set of voxels circling the fluid. If a voxel of the calculation field happens to be adjacent to a physical limit, corresponding discrete equations have non-defined terms (as, for example, $(u,v,w,T,P)_{i+1,j,k}$ for a voxel of (i,j,k) coordinates having a vertical wall on its right side). These terms are defined according to the expected effect upon the wall (bouncing, bursting, heating up, …) by applying conditions to the limit, be it Dirichlet's (in value) or Neumann's (in derivative). Choice is made here as : (i) fixing temperature values all around the calculation field at each time step, (ii) updating the pressure values to the limits by the pressure value located in the adjacent fluid voxel, thus making the pressure derivative between fluid and wall equal zero, (iii) applying Neumann's conditions in velocity, to describe the fluid's behaviour against the wall, while respecting (5). We shall choose, for example for a vertical wall, to define velocity at the limit, as the velocity contained in the adjacent fluid voxel by changing the sign of the y component (slip wall).

3.3 Problems of numerical stability and solution form

Explicit schemes such as (10) are said conditionally steady, because they must rigorously respect the criteria given by numerical analysis, in order not to diverge [5]. Characteristics of the fluid constants of (6)-(9) equations have been chosen from experimental data [4]. In this case, the solution presented in 3.2. happens to be laminar and visual interest happens to be limited. Lots of methods have been developping for the last 30 years, in order to study the turbulent flow of a fluid [7]. More complementary than rival, the most widespread methods are probably those of energy-dissipation type [8]. The appearance of turbulence in rather low velocites can be influenced by external forces (Archimedes' forces, Coriolis' forces…), by random limits conditions… However, the NS equations are supposed to "contain" turbulence. From which some research works directed towards direct resolution of these equations for a turbulent solution. Mechanics of fluids describe the range of turbulence by the dimensionless magnitude called Reynolds' number (noted Re). It is proportional to the fluid's velocity, as well as to the size of the walls within which it moves around. It is inversely proportional to the fluid's viscosity. The greater Re is, the more developped the turbulence is (i.e. more eddy scales are taken into account). The largest eddies are always of about the size of the walls and they strongly depend on the conditions to the limits. Direct numerical resolution of (5)-(8) in turbulent flow is generally limited to rather low Reynolds' numbers ($Re < 100$). Equations are the same for a liquid or a gas with low velocity and with reasonable temperature gradients. For example, experimental aerodynamics take a water flow (which is not very compressible) into consideration, rather than a wind tunnel, because water's viscosity (which is far less important than the air) allows to decrease the fluid's velocity for similar turbulence effects. Simulation enables to reduce viscosity (different fluid), in order to increase Re, but numerical stability criteria shall then impose the reducing of velocity in a significant way (for instance, Nick Foster [2] is limited to speeds of about $3 m.s^{-1}$). Unlike [2], we are sticking to the characteristics of simulated fluid and we choose to increase Re by considering high instantaneous velocities. The method presented hereabove shall not allow the solving of NS equations in this case. We suggest another solution.

4. ANOTHER APPROACH FOR MORE STABILITY

Numerical analysis might bring very easy methods for resolving PDE (see 3.2), it nevertheless proposes extraordinarily complex methods for solving really specific problems, with its discretization sometimes exceeding order 6. For a convection's generic calculation code, order 2 is enough. All these methods amount to consider an algebraic system at each time step. In this section, we develop a new method in 4.2 for more stability in practice, based on an implicit scheme.

4.1 A steady time discretization

A gain in stability is usually obtained by the implicit schemes that are interestingly quite often unconditionally steady. The simplest method of time integration is the implicit Euler method :

$$Q^{n+1} = Q^n + \Delta t \Psi\left(Q^{n+1}\right) \qquad (12)$$

Intuitively, this discretization appears to be better than its explicit homologue (10), because it anticipates (via the derivative) the $(n+1)\Delta t$ time solution. It better represents the fluid's time evolution, by requiring convergence towards a solution for each Δt. In fact, scheme (10) confounds physical time with iterations of the resolution, which is right if Δt is infinitely small… We can here solve pressure as previously, but for solving velocity, (6d)-(9d) equations shall consider f_u, f_v, f_w and f_T functions at $n+1$ time step. Right hand sides of equations, thus containing unknowns, induce convergence for each of them at each time step. If (12) authorizes some flexibility on convergence criteria, it is always possible to make the system diverge, in case time step shall not be small enough for important speed gradients. The bisectrix method proposes to increase this flexibility.

4.2 Bisectrix method

We suppose that the approximate solution between two successive time values is an arc of a circle. On *figure 3* : point M is Q's known solution at $n\Delta t$ time, point N is Q's sought solution at $(n+1)\Delta t$ time, C is the center of the circle, R is the radius, $\vec{\Psi}_E$ and $\vec{\Psi}_I$ are the tangential vectors to the circle, respectively in M and in N points, of respective coordinates :

$$\vec{\Psi}_E \left| \begin{array}{l} \Delta t \\ \Delta t \Psi\left(Q^n\right) \end{array} \right. \qquad \vec{\Psi}_I \left| \begin{array}{l} \Delta t \\ \Delta t \Psi\left(Q^{n+1}\right) \end{array} \right.$$

Point E thus represents Q's solution at $(n+1)\Delta t$ time, which is obtained according to the explicit scheme (10). Point I represents the solution, which is obtained according to the implicit scheme (12). If β is the angle between the two radii CM and CN, then (by orthogonallity) β is the angle between $\vec{\Psi}_E$ and $\vec{\Psi}_I$, and the MN chord, which leads to the sought solution, is then their bisectrix ($\alpha = \beta/2$) represented by $\vec{B}$ vector.

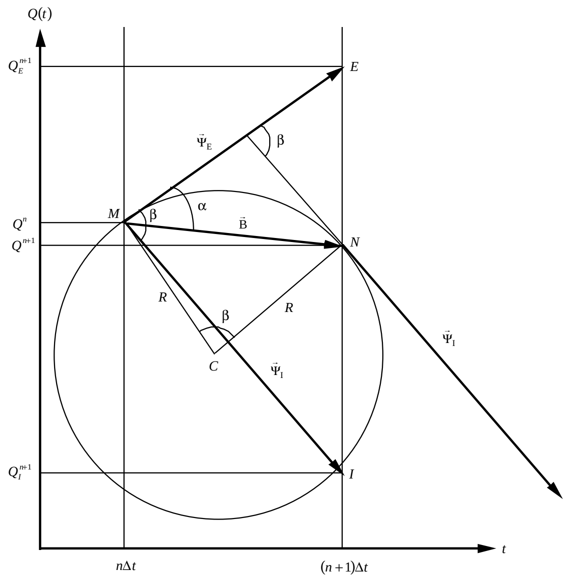

Figure 3. Bisectrix method

Point M being known, point N is easily determined from the coordinates of vector $\vec{B}$. The sum of $\vec{\Psi}_E$ and $\vec{\Psi}_I$ normed vectors provides the sought direction, and a forced displacement of Δt on the time axis provides length. From which :

$$\vec{B} \left| \begin{array}{l} \Delta t \\ \Delta t \dfrac{\Psi\left(Q^n\right)\sqrt{1+\Psi^2\left(Q^{n+1}\right)} + \Psi\left(Q^{n+1}\right)\sqrt{1+\Psi^2\left(Q^n\right)}}{\sqrt{1+\Psi^2\left(Q^{n+1}\right)} + \sqrt{1+\Psi^2\left(Q^n\right)}} \end{array} \right.$$

Thus, if one of the two vectors $\vec{\Psi}_E$ or $\vec{\Psi}_I$ has got an infinite slope, or if the two vectors have got an infinite slope, but of opposite sign, then the slope of the bisectrix is finite and calculation remains steady. We have implemented an implicit code based on (12) for which, at each time step, the first iteration shall give $\Psi\left(Q^n\right)$ and convergence shall give $\Psi\left(Q^{n+1}\right)$, the Q^{n+1} solution results of it.

4.3 The results obtained

The bisectrix method remains steady by taking larger time steps, in comparison with the two other methods and considering higher velocities. It allows hypersonic speeds, but the sense of the results is only mathematical, because in their physical interpretation, the (5)-(9) equations are not enough for such outflows. The results (hereunder) are obtained for laminar and turbulent flows. They take into consideration an enclosure (except at the inlet of the jets) with constant limits conditions. *Fig. 4*a represents velocity and temperature fields of a vortex; the wall on the left side heats the surrounding air, which rises and gets replaced by colder air that is heating itself in its turn… *Fig. 4*b represents the double vortex that has been obtained by ground heating. Following images on *fig. 4*c show a horizontal laminar warm jet, and *fig. 4*d shows two warm vertical sprigs. We must not see there any turbulences (Re=5). But with variable limit conditions (air currents, etc…), it becomes to enlarge twirls, to distort them…

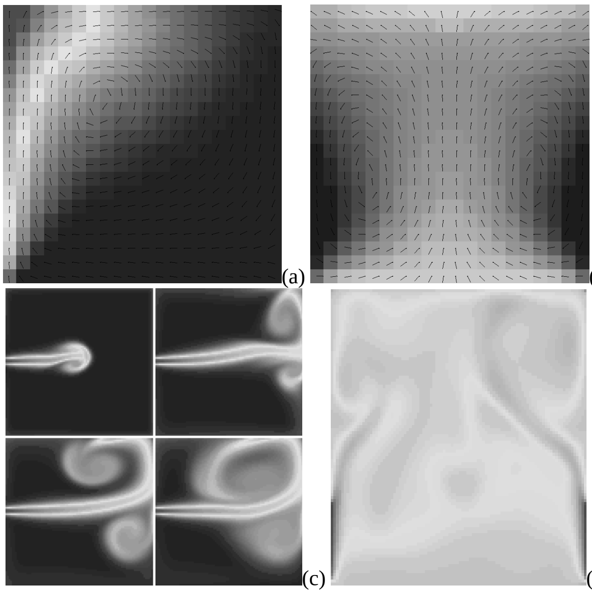

Figure 4. Re=5

Following images on *fig. 5* show a turbulent jet (Re=100 $\approx$ turbulence which is equivalent to that of the smoke of cigarette) and shall underline sinusoidal transition towards turbulence. Observe the expected appearance of a Karman street [9], the characteristical sea-horse, which is visible on the 5th image.

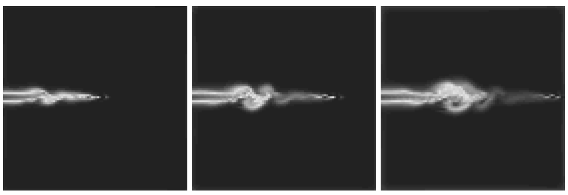

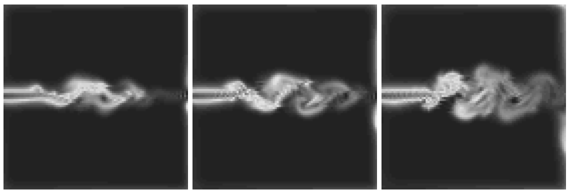

Figure 5. Re=100

Following are three images of the same jet, which is more powerful :

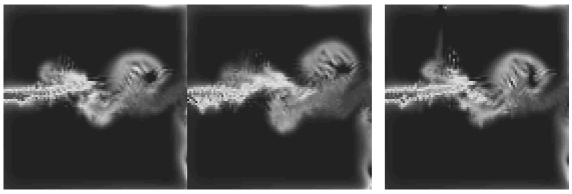

Re=1000 Re=10000

5. RENDERING THROUGH HEAT AND VISUALIZATION OF THE CONVECTIVE MOTIONS

Fig. 4 and *fig. 5* show velocity and temperature fields resulting from numerical data coming from the resolution of the (5)-(9) equations system. We can integrate these data in any classical method of rendering (ray-tracing, particles' systems…) in order to generate optical effects such as : disturbed vision through the heat, creation of mirages, etc… Jos Stam [10] presents stochastic functions on the refractive index of the air, and Marc Berger [11] considers the horizontal superposed air strata, for which the refractive index is fixed in an empirical manner. As for us, we include our convection voxmaps within our scenes. We have implemented a ray-tracing taking into account participating media [12] with absorption and diffusion phenomena. When a ray (coming from the eye) crosses a heat voxmap, it is deflected at each voxel according to temperature, which modifies the refractive index. The Lorenz-Lorentz law links refractive index n, density ρ, and molecular mass M of an ideal gas, according to $M(n^2-1)/(n^2+2)=\rho C$ where C is a constant. By considering density as the mass of the gas divided by the corresponding volume, and by applying the equation of ideal gases, the expression of ρ, obtained and combined to the Lorenz-Lorentz law, shall give for n :

$$n=\sqrt{\frac{1+2\delta T}{1-\delta T}} \qquad (13)$$

with $\delta = N^2 N_a R\beta_L / P$, where β_L is the constant of the Lorenz-Lorentz law - known for certain gases -, N the number of moles that are contained within the gas volume, N_a the Avogadro number, and R the constant of ideal gases. The curve of (13) for the air between 0° and 100°C is nearing a line, from wich the usual approximation by $n = aT$, by taking $a = 0.0036618342$; we get an index of 1.00023 at a temperature of 273.15°K (0°C). The *fig. 6* images show an experimentation that was made at the beginning of the century, in order to visualize convective motions : on the table, a container which is heated from under, is lighted by a light-spot; a shadow is casted on the wall. This is due to the fact that the hotter the water is, the less dense it is, and the less it refracts light. On *figure 6*a, the container is empty and one can see - normally - the corner of the room through it. On *fig. 6*b, it contains a voxmap of 49x59x7 voxels equivalent to *fig. 4*b : the vision through the container is disturbed, because rays were deflected at each voxel, according to the approximation of the Lorenz-Lorentz law. We can also observe the distortion of the shadow of the container's right pillar, through the fluid. We can visualize on the wall convective motion via an empirical coefficient on the temperature of each crossed voxel straight from the wall to the light-spot. *Fig. 6*c (front-view) considers boiling water, and *fig. 6*d is a section of the corresponding voxmap. We shall find here again the mirage effect: we cannot see the extremity of the table through the container, because rays are redirected upwards, according to the high temperature, and they shall render an image of the wall. Temperature gradients are higher up than down, and we can notice some voxels on the wall (no smoothing). Next scene (*fig. 7*) takes place in a chapel : the image of the stained glass window is projected on the oblique piece of wall as well as on the ground, participating medium is classical. On a pedestal to the left along the column, in a small dish, we have put a convection voxmap that we can visualize in tranparency. The density of a voxel is as a function of its temperature, and its empirically chosen spectrum (also function of temperature), shall imitate that of fire or that of fume. There is a light point source in each voxel of the flame (only one on *fig. 7*) which lightens the scene and we can see different illuminations on the walls due to the rims of the dish. We may think of simulating the movement of shadows in a dark room enlightened by a flickering flame, but the result shall be more interesting in a global illumination model [1] considering several light voxel sources... Finally, *figure 8* shows a scale full 3D particular version of Noah's Ark, using the same type of rendering. A 64x8x16 voxmap corresponding to a warm and powerful jet was placed behind the ship and the obtained fume looks like combustion gases.

6. CONCLUSION

This work offers a little state of the art on fluids mechanics and more particularly on theoretical thermal convection. It presents the usual methods for solving the related equations and proposes a steadier one, the bisectrix method, which especially authorizes larger time steps and higher velocities. We may consider very powerful jets, but we do not take into account compressibility of the fluid or shock waves… We finally visualize our scenes through the obtained heat voxmaps and we show three-dimensional convective motions under the shape of fume. If we wanted to go further in simulating fire motions (combustion), we could consider multi-kinds NS equations, adding chemical reaction equations to the system in the compressible case.

7. REFERENCES

[1]B. Battaille, D. Greenberg, K. Torrance, C. Goral. "Modeling the Interaction of Light between Diffuse Surfaces". Computer Graphics. Vol. 18, n°3, 1984, pp 213-222

[2]N. Foster, D. Metaxas. "Modeling the Motion of a Hot, Turbulent Gas". Siggraph 1997, Los Angeles, August 3-8, 1997. pp 181-188

[3]F. H. Harlow, J. E. Welch. "Numerical Calculation of Time-Dependent Viscous Incompressible Flow of Fluid with Free Surface". The Physics of Fluids Vol. 8, n°12, December 1965, pp 2182-2189

[4]A. Bejan. "Convection Heat Transfer 2nd Edition". Wiley, 1995

[5]C.A.J. Fletcher. "Computational Techniques for Fluid Dynamics 2nd Edition". Springer-Verlag, 1990

[6]P.G. Ciarlet, J.L. Lions. "Handbook of Numerical Analysis Vol. 1". North-Holland, 1990

[7]R. Schiestel. "Modélisation et simulation des écoulements turbulents". Hermes, 1993

[8]B. Mohammadi, O. Pironneau. "Analysis of the K-Epsilon Turbulence Model". Wiley, 1994

[9]M. Lesieur. "Turbulence in Fluids 2nd Edition". Kluwer, 1990

[10]J. Stam, E. Languenou. "Ray Tracing in Non-Constant Media". Proceedings of the Eurographics Workshop in Porto, Portugal, June 17-19, 1996, pp 225-234

[11]M. Berger, N. Levit, T. Trout. "Rendering mirages and other atmospheric phenomena". Eurographics '90, Montreux - Switzerland, 3-7 September, 1990, pp 459-468

[12]A. Watt. "3D Computer Graphics 2nd Edition". Addison-Wesley, 1993

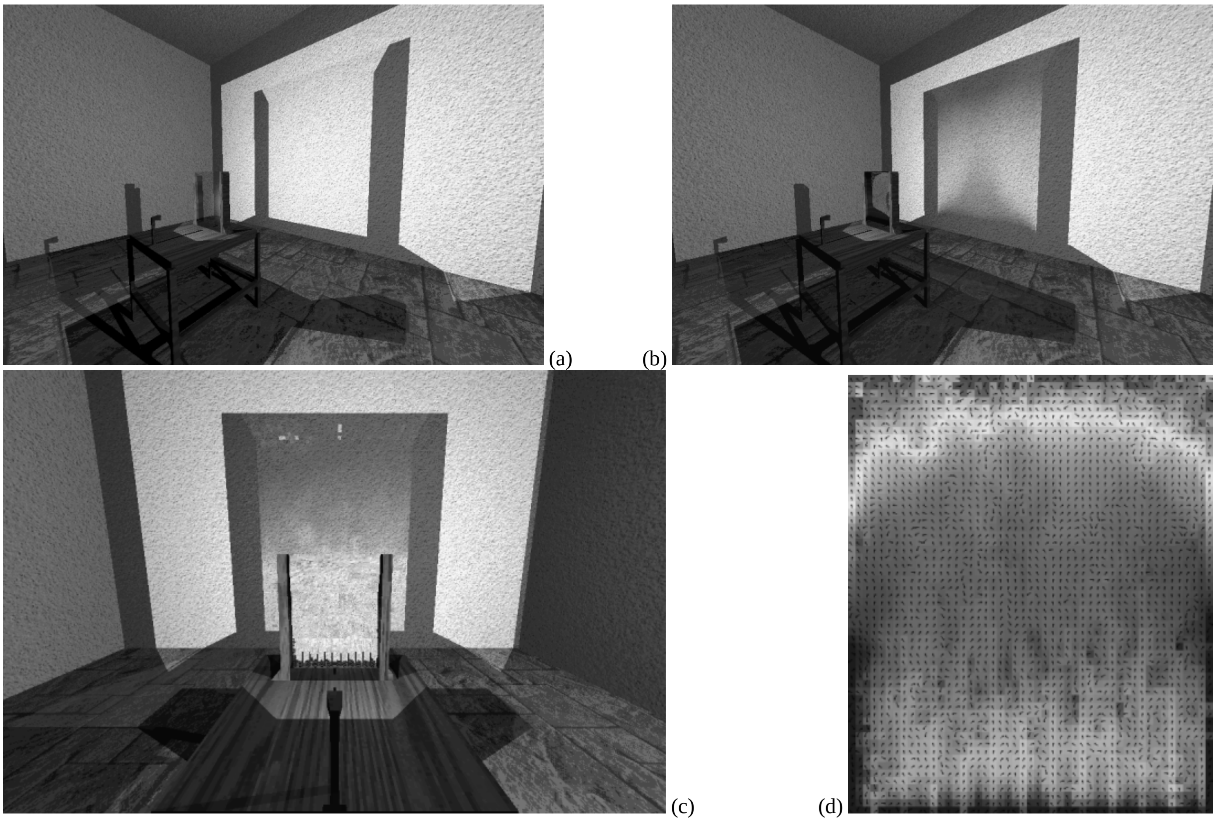
(a) (b) (c) (d)

Figure 6. Convection currents

Figure 7. Smoky chapel

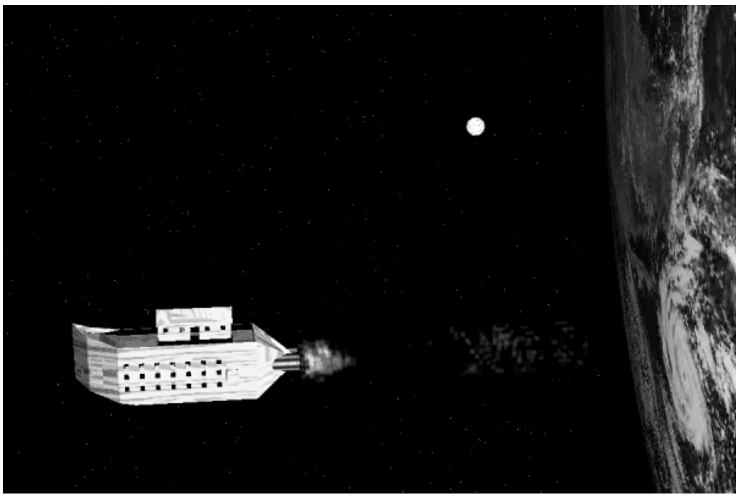

Figure 8. Noah's escape